JHEP

Published for SISSA by Springer

Received: *June 24, 2016*
Accepted: *August 3, 2016*
Published: *August 11, 2016*

tbW anomalous couplings in the Two Higgs Doublet Model

Abdesslam Arhrib and Adil Jueid

Département de Mathématiques, Faculté des Sciences et Techniques,
Université Abdelmalek Essaadi,
B. 416, Tangier, Morocco

E-mail: aarhrib@gmail.com, ajueid@ictp.it

Abstract: We make a complete one loop calculation of the tbW couplings in the Two Higgs Doublet Model. We evaluate both the anomalous couplings g_L and g_R as well as left handed and right handed component of tbW. The computation is done in the Feynman gauge using the on-shell scheme renormalization for the Standard Model wave functions and parameters. We first show that the relative corrections to these anomalous couplings are rather small in most regions of the parameter space. We then analyze the effects of these anomalous couplings on certain observables such as top quark polarization in single top production through $t-$channel as well as $W^{\pm}$ boson helicity fractions in top decay.

Keywords: Beyond Standard Model, Heavy Quark Physics

ArXiv ePrint: 1606.05270

doi:10.1007/JHEP08(2016)082

JHEP08(2016)082

Contents

JHEP08(2016)082

1 Introduction

Top quark is the heaviest particle discovered by D0 [1] and CDF [2] collaborations at the Tevatron-Fermilab with mass $m_t = 173.21 \pm 0.51(stat.) \pm 0.71(syst.)$ GeV. Some of its properties have been studied by the first run of LHC and will get improved by the new LHC run. It is well known that LHC machine with 13-14 TeV center of mass energy will act as a top factory since the total cross section for top quark pair production will reach one nanobarn. At the LHC, the top quark production will be two orders of magnitude larger than in the Tevatron. At low luminosity phase of LHC, one expects about ten millions top pairs per year and this number will increase during the high luminosity phase. Therefore, with such extremely large number of top anti-top, it is expected that top quark properties (top mass, top spin and decay rates...) can be examined with very good precision.

The main decay of the top quark is into W boson and bottom quark. At the tree level, this decay proceeds through the left handed V-A charged weak interaction which is directly proportional to Cabbibo-Kobayachi-Maskawa V_{tb} that can be measured in single top production. Both in the Standard Model (SM) and Beyond SM, loop effects can modify the structure of tbW vertex. Such modifications are typically described by anomalous couplings g_L and g_R as well as modifications to left handed (V_L) and right handed (V_R)

components of tbW. The QCD corrections to the anomalous coupling g_R have been evaluated a while ago in [3], while the SM electroweak and QCD corrections to $g_{L,R}$ and V_R have been studied in [4] and [5]. It turns out that the anomalous couplings g_L, g_R as well as top quark right coupling g_R in the tbW are dominated by the QCD corrections.

It is well known that, the anomalous tbW couplings could be probed by measuring the W boson helicity fractions in the top quark decay [6, 7]. These polarization states are proven to be sensitive to new physics effects [8]. Moreover, top quark due to its short lifetime, decays before it hadronizes. Therefore, the information about its polarization may be preserved in its decay products which can be viewed as top spin analyzers.

In this study, we are interested in computing the complete one loop contribution to the anomalous tbW couplings in the framework of Two Higgs Doublet Model (2HDM). We evaluate both the anomalous couplings g_L and g_R as well as left handed V_L and right handed V_R component of tbW. We stress that, evaluation of the top anomalous couplings in the framework of the two Higgs Doublet Model (2HDM) has been studied some times ago in [9] and recently in [10]. In [10], only the computation of the tensorial anomalous couplings g_R and g_L has been considered. We will perform, in addition to tensorial couplings $g_{L,R}$, a complete one-loop computation of the left and right chiral couplings V_L and V_R and quantify their effects on top quark polarisation in single production through t-channel and $W^{\pm}$ helicity fractions.

The 2HDM effects are found to be below percent level. In the present computation, we perform a comparative study and will include all the virtual effect of the 2HDM as well as the real emission of photon and gluon in the final state that are necessary for the computation of the one loop contribution to V_L in order to have infra-red finite result.

There have been several experimental searches for anomalous coupling of the top quark. One of the most strongest constraints comes from measurement of $Br(\bar{B} \to X_s\gamma)$ [11]. Tevatron also has reported limits on the anomalous couplings in the search of new physics in top quark decays [12]. We note also that there are limits from ATLAS and CMS collaborations on anomalous couplings from the measurements of the $W^{\pm}$ helicity fractions in top quark decay [6, 7]. In this regard, the first measurement was reported by the CMS collaboration [13] assuming $V_L = 1, g_L = V_R = 0$, they have found the following value $g_R = 0.070 \pm 0.053(stat.)^{+0.081}_{-0.073}(syst.)$. But this measurement suffers from large statistical and systematic uncertainties. The sensitivity of the ATLAS experiment to the anomalous tbW couplings has been studied in [14]. Finally, we stress here that the anomalous couplings might be measured from the measurement of single top production cross section at the LHC [15], from the measurements of Laboratory frame observables constructed in [16] through single top production at the LHC [17], and from the observables that were considered for the case of a future e^-p collider [18].

In fact, all measurements of top quark properties performed so far are in perfect agreement with the SM theoretical predictions. We would like to investigate the top quark tbW anomalous couplings as well as left and right handed tbW couplings in the 2HDM, and quantize their effects on some top quark observables such as top polarization in single top production through $t-$channel as well as $W^{\pm}$ helicity fractions in top decay.

JHEP08(2016)082

The outline of this paper is the following: in section 2, we introduce the two Higgs Doublet Model, its parameters and the constraints that we will use during the numerical analysis. In section 3, we describe the experimental status of the anomalous couplings and the theoretical set-up used in our calculation while in section 4, we present and discuss our numerical results. Our conclusions are drawn in section 5. The appendix is devoted to analytical expression for the one-loop anomalous couplings given for the first time in terms of Passariono-Veltman functions and comparison with some results from literature.

2 The Two-Higgs-Doublet-Model

In the Two-Higgs-Doublet Model, two scalar doublets under $SU(2)_L$ with Hypercharge $Y_{H_{1,2}} = 1/2$ are used to generate fermion and gauge boson masses. The inclusion of the two doublets may give rise to sizeable flavor changing neutral current processes (FCNC) at tree level. In order to avoid such tree level FCNC, a discrete symmetry Z_2 (for example $H_1 \to H_1$ and $H_2 \to -H_2$) is imposed [19]. Hence, there are 4 different combinations of the Yukawa Lagrangian depending on the Z_2 charge assignment to the leptons and quarks fields [20, 21]. There are four different models of Yukawa interactions. In type-I model, only the second doublet H_2 interacts with all the fermions while in type-II model where the doublet H_2 interacts with up-type quarks and H_1 interacts with the charged leptons and down-type quarks. In type-X model, charged leptons couple to H_1 while all the quarks couple to H_2. Finally, in type-Y model, charged leptons and up-type quarks couple to H_2 while down-type quarks acquire masses from their couplings to H_1. Given that the Higgs couplings to quarks are the same in type-I (resp type-II) and in type-X (resp type-Y), in what follow we will discuss only 2HDM type-I and II.

The Lagrangian representing the Yukawa interactions is given by:

$$-\mathcal{L}_{Yuk} = \bar{q}_L \mathcal{Y}_u \widetilde{H}_2 u_R + \bar{q}_L \mathcal{Y}_d H_d d_R + \bar{l}_L \mathcal{Y}_l H_l l_R + \text{H. c}, \tag{2.1}$$

where $H_i, i = l, d$ is either H_1 or H_2 and $\mathcal{Y}_i$ is a set of Yukawa matrices.

The most general scalar potential which is gauge-invariant, re-normalizable and CP-invariant is:

$$\begin{aligned} V(H_1, H_2) = &\mu_{11}^2 |H_1|^2 + \mu_{22}^2 |H_2|^2 - \mu_{12}^2 (H_1^\dagger H_2 + H_2^\dagger H_1) + \lambda_1 |H_1|^4 + \lambda_2 |H_2|^4 + \lambda_3 |H_1|^2 |H_2|^2 \\ &+ \lambda_4 |H_1^\dagger H_2|^2 + \frac{\lambda_5}{2} [(H_1^\dagger H_2)^2 + \text{H.c}], \end{aligned} \tag{2.2}$$

with $\mu_{11,22}^2, \lambda_{i,(i=1\ldots4)}$ are real parameters while μ_{12}^2 and λ_5 could be complex for CP violating case. Note that in the above potential the Z_2 symmetry is only broken softly by dimension 2 term $\mu_{12}^2 (H_1^\dagger H_2)$ while dimension four terms are not introduced in our potential. The two Higgs doublets H_1 and H_2 are given by:

$$H_i = \begin{pmatrix} \phi_i^+ \\ v_i + \frac{1}{\sqrt{2}}(h_i + i\omega_i) \end{pmatrix} \qquad , i = 1, 2, \tag{2.3}$$

where v_1 and v_2 are the vacuum expectation values of the two doublets. After electroweak symmetry breaking, one has five additional degrees of freedom; a pair of charged scalar

JHEP08(2016)082

	κ_u^h	κ_d^h	κ_l^h	κ_u^H	κ_d^H	κ_l^H	κ_u^A	κ_d^A	κ_l^A
Type-I	c_α/s_β	c_α/s_β	c_α/s_β	s_α/s_β	s_α/s_β	s_α/s_β	c_β/s_β	$-c_\beta/s_\beta$	$-c_\beta/s_\beta$
Type-II	c_α/s_β	$-s_\alpha/c_\beta$	$-s_\alpha/c_\beta$	s_α/s_β	c_α/c_β	c_α/c_β	c_β/s_β	s_β/c_β	s_β/c_β
Type-X	c_α/s_β	c_α/s_β	$-s_\alpha/c_\beta$	s_α/s_β	s_α/s_β	c_α/c_β	c_β/s_β	$-c_\beta/s_\beta$	s_β/c_β
Type-Y	c_α/s_β	$-s_\alpha/c_\beta$	c_α/s_β	s_α/s_β	c_α/c_β	s_α/s_β	c_β/s_β	s_β/c_β	$-c_\beta/s_\beta$

Table 1. Yukawa couplings in terms of mixing angles in the 2HDM Type I, II, X and Y.

bosons $H^\pm$, one CP-odd A^0 and two CP-even h^0, H^0 where the lightest CP-even scalar boson is identified as the SM Higgs boson. These eigenstates are defined as follow:

$$\begin{pmatrix} h_1 \\ h_2 \end{pmatrix} = O(\alpha) \begin{pmatrix} H^0 \\ h^0 \end{pmatrix}, \quad \begin{pmatrix} \phi_1^\pm \\ \phi_2^\pm \end{pmatrix} = O(\beta) \begin{pmatrix} G^\pm \\ H^\pm \end{pmatrix}, \quad \begin{pmatrix} \omega_1 \\ \omega_2 \end{pmatrix} = O(\beta) \begin{pmatrix} G^0 \\ A^0 \end{pmatrix} \tag{2.4}$$

where: $O(\theta) = \begin{pmatrix} \cos\theta & -\sin\theta \\ \sin\theta & \cos\theta \end{pmatrix}$.

The Yukawa Lagrangian in eq. (2.1) becomes:

$$\begin{aligned} -\mathcal{L}_{Yuk} = \sum_{\psi=u,d,l} \Big(\frac{m_\psi}{v} \kappa_\psi^h \bar{\psi}\psi h^0 + \frac{m_\psi}{v} \kappa_\psi^H \bar{\psi}\psi H^0 - i \frac{m_\psi}{v} \kappa_\psi^A \bar{\psi}\gamma_5 \psi A^0 \Big) + \\ \Big(\frac{V_{ud}}{\sqrt{2}v} \bar{u}(m_u \kappa_u^A P_L + m_d \kappa_d^A P_R) d H^+ + \frac{m_l \kappa_l^A}{\sqrt{2}v} \bar{\nu}_L l_R H^+ + H.c. \Big) \end{aligned} \tag{2.5}$$

where κ_i^S are the Yukawa couplings in the 2HDM. In table 1, we give the values of the couplings in the four types of Yukawa interactions of the 2HDM with softly broken Z_2 symmetry. We will identify the light CP-even Higgs h^0 as the 125 GeV SM Higgs, the other parameters of the 2HDM are not yet measured by any experiment, hence we will apply the following theoretical and experimental constraints on the parameter space of the model:

- Vacuum stability of the scalar potential [22].
- Tree-level perturbative unitarity [23–25].
- We imposed constraints on the ρ parameter using the PDG update on electroweak fits [26].
- We imposed constraints from the ATLAS measurement [27] of the signal strength μ_{XX} defined by:

$$\mu_{XX} = \frac{\sigma(pp \to h^0)^{\text{2HDM}} \Gamma(h^0 \to XX)^{\text{2HDM}}}{\sigma(pp \to h^0)^{\text{SM}} \Gamma(h^0 \to XX)^{\text{SM}}}, \tag{2.6}$$

  where XX represents the channels: $W^{\pm *}W^\mp, ZZ^*, \gamma\gamma$, and $\tau^+\tau^-$ and $\sigma(pp \to h^0)$ includes the Higgs production mechanisms at the LHC: ggF, VBF, $W^\pm h^0, Zh^0$ and $t\bar{t}h^0$.

JHEP08(2016)082

- We will use the results of indirect constraints on the charged Higgs boson mass from processes at the one-loop order, e.g $b \to s\gamma$ and R_b [28–35]. In our analysis, we assume that $m_{H^\pm} \geq 480\,\text{GeV}$ in 2HDM type-II.

- Constraints from direct searches of charged Higgs bosons at LEP [36] and the LHC [37–39] will be used.

3 Anomalous *tbW* couplings

Owing to Lorentz invariance, the amplitude of top quark decay $t(p_t) \to b(p_b)W^+(q)$ can be written as:

$$\mathcal{M}(t \to bW^+) = \frac{-e}{\sqrt{2}\sin\theta_W}\bar{u}_b\left[(V_L P_L + V_R P_R)\gamma^\mu + \frac{i\sigma^{\mu\nu}q_\nu}{M_W}(g_L P_L + g_R P_R)\right]u_t\epsilon^*_\mu, \tag{3.1}$$

where $P_{R,L} = \frac{1}{2}(1 \pm \gamma_5)$ are the projection operators, p_t, p_b and $q = p_t - p_b$ are respectively the four-momenta of the top, bottom and W^+ boson. The three particles are assumed to be on-shell. For the case of W^+ being off shell, there are two-additional terms which should be added to the matrix elements[1] in eq. (3.1). At tree level, in the SM, $V_L = V_{tb}$ and $V_R = g_R = g_L = 0$, while radiative corrections in the SM induce non-zero values for V_R, g_R and g_L. Note that renormalizable theories beyond the SM might induce non-zero values for the right chiral coupling V_R even at tree level, but g_R and g_L have to be induced only at one-loop order. Before discussing the details of our calculations, we recapitulate the experimental status of the direct searches for the anomalous couplings as well as the indirect constraints coming from one-loop induced processes.

One of the strongest constraints comes from $\text{BR}(\bar{B} \to X_s\gamma)$ [11]. The enhancement factor m_t/m_b implies that these constraints are stronger for V_R and g_L and rather weaker for g_R:

$$\begin{aligned} -0.15 \leq \text{Re}(g_R) \leq 0.57, \\ -7 \times 10^{-4} \leq V_R \leq 2.5 \times 10^{-3}, \\ -1.3 \times 10^{-3} \leq g_L \leq 4 \times 10^{-4}. \end{aligned} \tag{3.2}$$

There are also 2σ limits available for $g_{L,R}$ using LHC simulations [40];

$$-0.026 < g_R < 0.024 \quad \text{and} \quad -0.058 < g_L < 0.026\,.$$

In the search of new physics in top quark decays [12], Tevatron has reported 95% CL limit on anomalous couplings as follow:

$$|V_R|^2 < 0.30\,, \qquad |g_L|^2 < 0.05 \quad \text{and} \quad |g_R|^2 < 0.12. \tag{3.3}$$

It was assumed $V_L = V_{tb}$.

[1] In other words, two form factors f_L and f_R have to be added as follows $\bar{u}_b(p_b)\frac{i\sigma^{\mu\nu}(p_t+p_b)_\nu}{M_W}(f_L P_L + f_R P_R)u_t(p_t)\epsilon^*_\mu(q)$.

There are also 95% CL limits [41] on all the anomalous couplings that appear in eq. (3.1) from a global fit to experimental data. This data includes single top production cross section (t-channel, s-channel and tW associated production) and $W^{\pm}$ helicity fraction at both the Tevatron and the LHC. These limits are:

$$\begin{aligned} -0.142 \leq g_R \leq 0.023\,, \qquad & -0.081 \leq g_L \leq 0.049, \\ 0.902 \leq V_L \leq 1.081 \quad \text{and} \quad & -0.112 \leq V_R \leq 0.162. \end{aligned} \tag{3.4}$$

Moreover, a global fit of the anomalous Wtb couplings has been performed in [42] where correlations among the different effective operators have been investigated.

On the other hand, limits on tensorial anomalous couplings g_L and g_R have been studied in [44, 45] by combining several constraints from $b \to s\gamma$, helicity fractions, single top production, electroweak precision test (mainly from the S-parameter) and the electric dipole moments. It was found that the real part of g_R is strongly constrained by the helicity fractions while the strongest constraint on $\mathrm{Re}[g_L]$ comes from $b \to s\gamma$ branching ratio. On the other hand, the imaginary part of tensorial couplings is severely constrained by the electric dipole moments (EDM); e.g the strongest constraint on $\mathrm{Im}[g_L]$ comes from neutron EDM while $\mathrm{Im}[g_R]$ is strongly constrained by electron EDM.

The ATLAS collaboration [43] has reported 95% CL limits on the ratios of the anomalous couplings g_R and V_L from the measurement of the double differential decay rate of the top quark in single top production through t-channel process at $\sqrt{s} = 7$ TeV taking $V_R = g_L = 0$. The limits are:

$$\mathrm{Re}\left[\frac{g_R}{V_L}\right] \in [-0.36, 0.10] \text{ and } \mathrm{Im}\left[\frac{g_R}{V_L}\right] \in [-0.17, 0.23] \tag{3.5}$$

Recently, ref. [46] puts 95% CL limits on the real and imaginary part of the anomalous couplings which were obtained from a global fit to data using the following observables:

- t-channel single top production cross section at the LHC at $\sqrt{s} = 7, 8$ and $13\,\mathrm{TeV}$ and at Tevatron $\sqrt{s} = 1.96\,\mathrm{TeV}$,
- s-channel tW associated production at both the LHC $7 \oplus 8\,\mathrm{TeV}$ and Tevatron
- Results from $W^{\pm}$ helicity fractions in $t\bar{t}$ production at $\sqrt{s} = 8\,\mathrm{TeV}$
- Expected results corresponding the t-channel production cross section at $\sqrt{s} = 14$ and $33\,\mathrm{TeV}$ assuming that $V_L = V_{tb} \simeq 1$.

We stress that these limits are rather weak for V_R, and g_L and slightly stronger for the case of g_R.

We will perform a complete analysis of all anomalous couplings present in eq. (3.1). The corresponding Feynman diagrams are depicted in figure 1. For the calculation of g_L, g_R and V_R, there is no need to renormalize the theory since these couplings are absent at tree level. In fact, infrared divergences are also absent in the case of these couplings. For instance, in the case of g_L and g_R, contributions from diagrams with exchange $tW^{\pm}\gamma$ and

JHEP08(2016)082

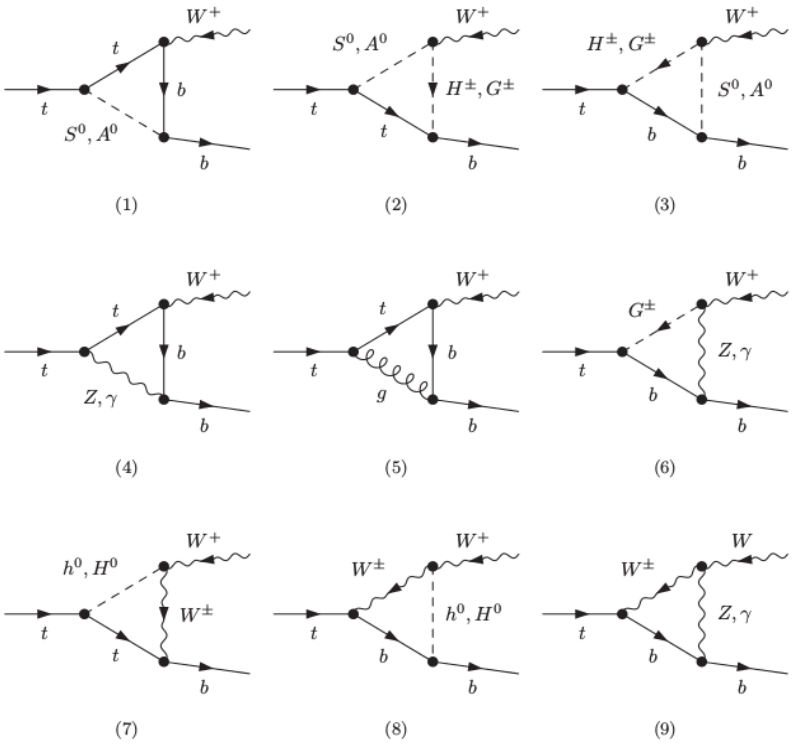

Figure 1. Feynman diagrams that contribute to one loop tbW coupling in the 2HDM.

$tG^{\pm}\gamma$ (from $bW^{\pm}\gamma$ and $bG^{\pm}\gamma$) are individually infrared divergent but their sum is infrared finite. On the other hand, in the case of V_R, all the diagrams involving the photon/gluon are IR finite.

Before computing the anomalous couplings in the framework of the 2HDM, we have calculated them in the SM and compared with the results of [4] for the case of g_L and g_R and with [5] for the case of the right chiral coupling V_R. The numerical values of g_L, g_R and V_R in the SM are tabulated in appendix A while their analytical expressions are given for the first time in terms of Passarino-Veltamn functions are shown in appendix B.

The one-loop correction to V_L involves divergent integrals. In order to get meaningful results, we should add appropriate counter-term to the bare coupling. In order to achieve that, we will be working in the on-shell renormalization scheme [47, 48], where necessary redefinition of the fields and parameters is performed such that the total amplitude (unrenormalized and counter term) is UV-finite. The counter-term of tbW coupling is given by:

$$\delta\mathcal{M}_{tbW} = \bar{u}_t(p_t) ie\gamma^{\mu} P_L \delta C_- u_b(p_b)\epsilon^*_{\mu}(q), \tag{3.6}$$

where δC_- is:

$$\delta C_- = \frac{1}{\sqrt{2}s_W}\left(\delta Z_e - \frac{\delta s_W}{s_W} + \frac{1}{2}\delta Z_W + \frac{1}{2}(\delta Z^{t,L\dagger} + \delta Z^{b,L})\right), \tag{3.7}$$

JHEP08(2016)082

where we have assumed that $V_{tb} = 1$ and $\delta V_{tb} = 0$. The renormalization constants $\delta Z_e, \delta s_W, \delta Z_W, \delta Z^{t,L\dagger}$ and $\delta Z^{b,L}$ are determined as usual by suitable mass and field renormalization conditions.

The Feynman diagrams and the corresponding amplitudes have been generated with FeynArts and FormCalc packages [50–53]. The output was passed to LoopTools [54–56] for numerical integration of the one-loop functions. UV divergences and renormalization scale independence have been checked analytically with FormCalc and numerically with LoopTools. However, due to the contribution of virtual photons and gluons, the corrections to V_L are infrared divergent. These IR divergences are cancelled after introducing real photons and gluons emissions in the final state. We have checked that indeed, the total amplitude consisting of virtual, soft and hard photons/gluons emissions are independent of the effective cutoff λ^2_{IR}. This cancellation has been checked analytically by computing the IR divergent of the three-points Passarino Veltman function C_0 in the soft limit using analytical expressions from [49] and the real (soft and hard) emission factors extracted from [48]. With LoopTools, we checked numerically that the total contribution:

$$2\mathrm{Re}(\mathcal{M}^*_{\mathrm{tree}}\mathcal{M}_{\mathrm{virtual}}) + |\mathcal{M}_{\mathrm{real}}|^2, \tag{3.8}$$

is independent of λ^2_{IR} by computing the sum (3.8) for different values of $\lambda^2_{IR} \in [10^{-10} : 10^6]$ and have found that the sum is λ^2_{IR} independent.

4 Numerical results

The input parameters of the SM are taken from the Particle Data Group [26]:

$m_t = 173.21\,\mathrm{GeV}$	$m_b = 4.66\,\mathrm{GeV}$
$M_W = 80.385\,\mathrm{GeV}$	$M_Z = 91.1876\,\mathrm{GeV}$
$\alpha_S = 0.118$	$m_H = 125\,\mathrm{GeV}$

while the parameter space of the 2HDM is scanned over the range specified in table 2.

For our numerical analysis, we define the following ratios $\Delta\mathcal{O}_i$:

$$\Delta\mathcal{O}_i = \frac{\mathcal{O}_i^{2HDM} - \mathcal{O}_i^{SM}}{\mathcal{O}_i^{SM}}, \tag{4.1}$$

with $\mathcal{O}_i = \mathrm{Re}(g_L), \mathrm{Re}(g_R), \mathrm{Re}(V_R)$ and $\mathrm{Re}(V_L) + V_{tb}$.

4.1 Anomalous couplings

The relative correction Δg_L is shown in figure 2 in different plan ($\tan\beta$, κ_d^h) (left panels), (m_H, m_A) (middle panels) and ($\sin(\beta-\alpha), \cos\alpha$). Upper panels are for 2HDM-I and lower panels for 2HDM-II. One can see that g_L gets enhancement for type-I (in most regions of the parameter space) while it is always suppressed with respect to the SM for 2HDM type-II. Most of the regions in the parameter space correspond to $\Delta g_L < 2\%$. In type-I, Δg_L reaches 3.5% for $\tan\beta \sim 1$ (left panel) and for all values of κ_d^h between 1 and 1.3 and

JHEP08(2016)082

Type-I	Type-II
$100\,\text{GeV} \leq m_{H^\pm} \leq 900\,\text{GeV}$	$480\,\text{GeV} \leq m_{H^\pm} \leq 900\,\text{GeV}$
$90\,\text{GeV} \leq m_{A^0} \leq 900\,\text{GeV}$	$90\,\text{GeV} \leq m_{A^0} \leq 800\,\text{GeV}$
$125\,\text{GeV} \leq m_{H^0} \leq 900\,\text{GeV}$	$125\,\text{GeV} \leq m_{H^0} \leq 900\,\text{GeV}$
$0 \leq \sin(\beta - \alpha) \leq 1$	$0 \leq \sin(\beta - \alpha) \leq 1$
$1 \leq \tan\beta \leq 30$	$1 \leq \tan\beta \leq 30$
$-25 \leq \lambda_5 \leq 25$	$-25 \leq \lambda_5 \leq 25$

Table 2. Parameter space of the Two-Higgs-Doublet model Type-I and -II over which the scan has been performed.

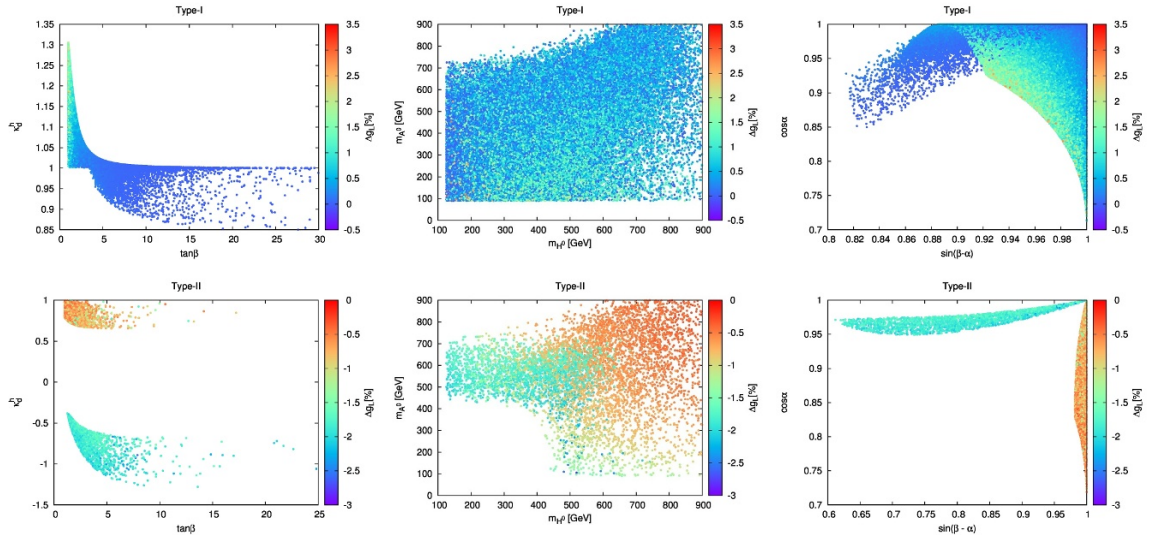

Figure 2. Relative contribution Δg_L in 2HDM type-I (upper panels) and type-II (lower panels) shown as a scatter plot in the $(t_\beta,\ \kappa_d^h)$ plan (left), (m_{H^0}, m_{A^0}) plan (middle) and $(s_{\beta-\alpha}, c_\alpha)$ plan (right).

also for $m_{H^0,A^0} \in [100 : 300]\,\text{GeV}$ (middle panel). A decoupling behavior is easily observed for large values of $\tan\beta \geq 25$, $\kappa_d^h \sim 1$ and also for heavy scalars $m_{A^0,H^0} > 700\,\text{GeV}$.

In 2HDM type-II, we see that Δg_L is always negative while it approaches 0%, (SM regime), for $\kappa_d^h \sim 1$ and $\tan\beta \sim 1$.

In figure 3, we plot the correction to g_R in type-I 2HDM (upper panels) and type-II 2HDM (lower panels). We can see that corrections in type-I model can reach -5% for $\tan\beta \sim 1$ and the enhancement attains 1%. However, in type-II 2HDM, the suppression of the correction to g_R with respect to the SM result is smaller and the enhancement is quite bigger than type-I 2HDM, i.e $\max \Delta g_R \simeq 1.5\%$ and $\min \Delta g_R \simeq -2\%$.

In figure 4 (upper panels), we illustrate the correction to V_R in 2HDM type-I. It is clear from these plots that the corrections hardly reach 2% while the maximum of suppression is about -3.5%. The decoupling limit where $V_R^{2HDM} = V_R^{SM}$ is attained for large $\tan\beta$, large masses $m_{H^0,A^0} > 700\,\text{GeV}$ and for $s_{\beta-\alpha} \simeq 1$.

JHEP08(2016)082

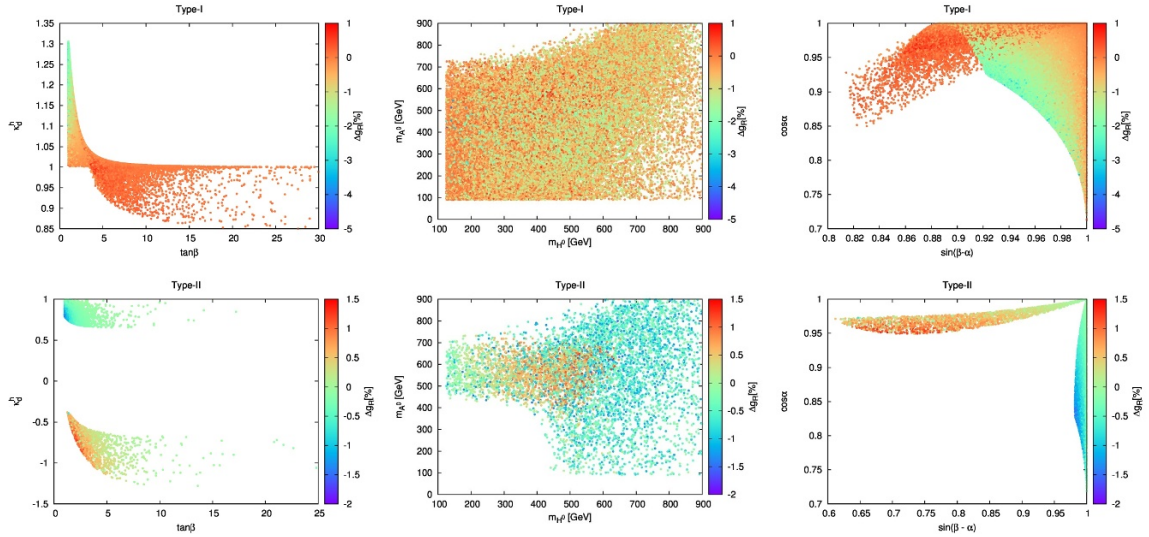

Figure 3. Relative contribution Δg_R in 2HDM type-I (upper panels) and type-II (lower panels) shown as a scatter plot in the $(t_\beta,\, \kappa_d^h)$ plan (left), (m_{H^0}, m_{A^0}) plan (middle) and $(s_{\beta-\alpha}, c_\alpha)$ plan (right).

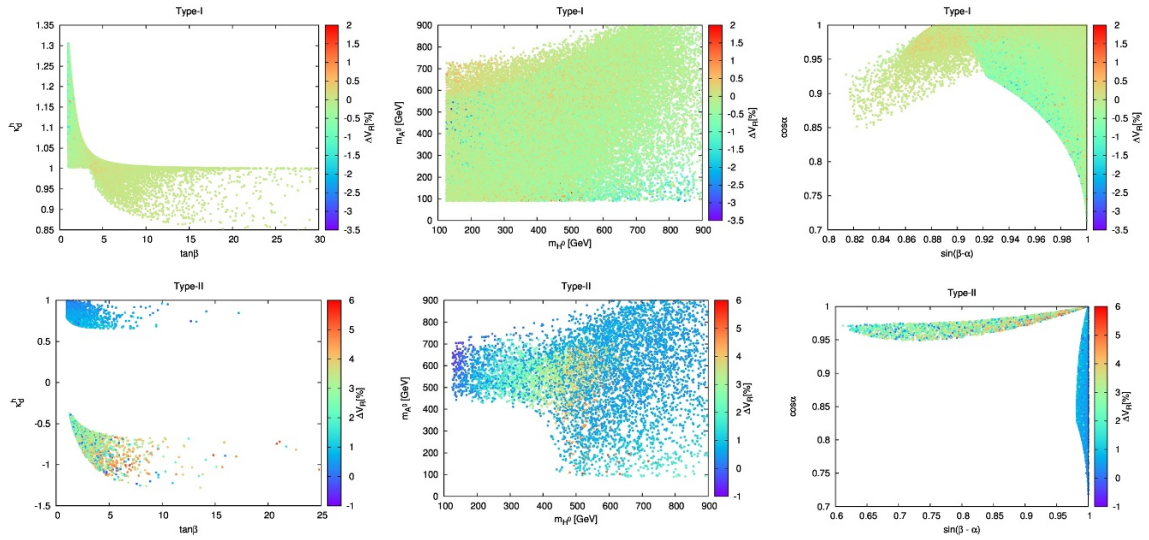

Figure 4. Relative contribution ΔV_R in 2HDM type-I (top) and 2HDM type-II (bottom) shown as a scatter plot in $(t_\beta,\, \kappa_d^h)$ plan (left), (m_{H^0}, m_{A^0}) plan (middle) and $(s_{\beta-\alpha}, c_\alpha)$ plan (right).

In the lower panels of figure 4, we can see that, contrarily to 2HDM type-I, the enhancement of V_R in 2HDM type-II is larger and reaches 6% for m_{H^0} and $m_{A^0} \in [300 : 400]$ GeV while the suppression is hardly fulfilled and reaches only -1%.

In figure 5, we have shown corrections to the left chiral coupling V_L. We see that the corrections are very small (not exceeding 0.4%) in most regions of the parameter space. The suppression of V_L with respect to its SM value reaches -0.5% in the 2HDM type-I and II.

JHEP08(2016)082

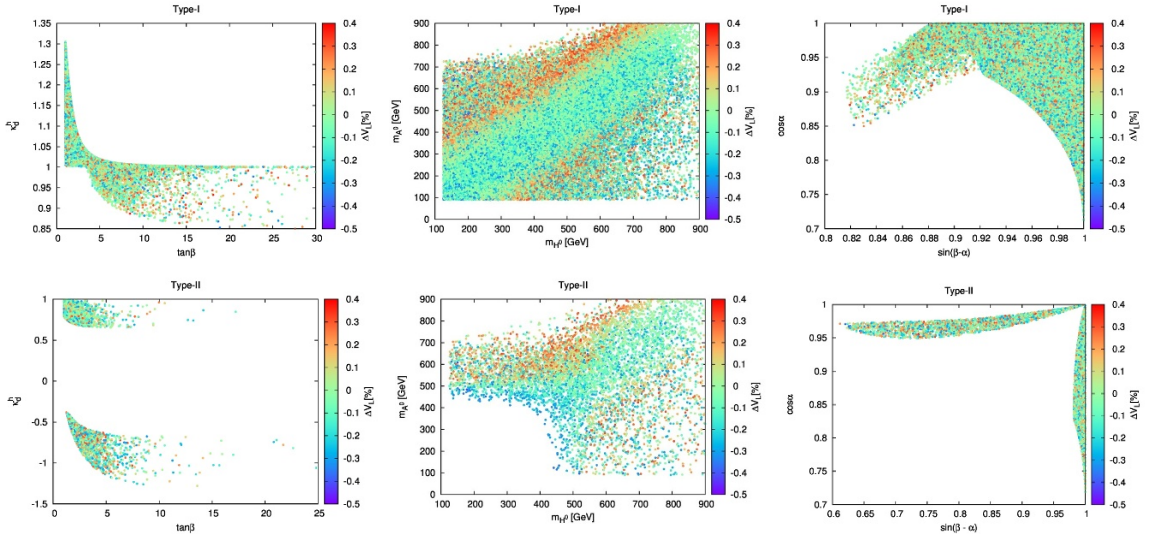

Figure 5. Relative contribution ΔV_L in 2HDM type-I (top) and 2HDM type-II (bottom) shown as a scatter plot in $(t_\beta,\, \kappa_d^h)$ plan (left), (m_{H^0}, m_{A^0}) plan (middle) and $(s_{\beta-\alpha}, c_\alpha)$ plan (right).

	Top quark	Anti-top quark
P_x	-0.0179074	-0.107771
P_y	0.0040848	9.66629×10^{-6}
P_z	0.880908	-0.850601

Table 3. Values of the polarization of $t/\bar{t}$ in the SM at $\sqrt{s} = 14\,\text{TeV}$. Formulae have been taken from ref. [59].

4.2 Top polarization

We also studied numerically the top polarization in the channel $qg \to q' t\bar{b}$ at the LHC for $\sqrt{s} = 14$ TeV. The relative correction is defined as:

$$\Delta P_i = \frac{P_i^{\text{2HDM}} - P_i^{\text{SM}}}{P_i^{\text{SM}}}\,, \qquad i = x, y, z \tag{4.2}$$

Following ref. [59], the axes are defined as; the z-axis is the direction of the spectator quark q', the y-axis is orthogonal to the direction of the momentum of the initial quark q and the momentum of the spectator quark q' and the x-axis is chosen such that the system is right handed. We have taken the expressions of the components of the polarization vector from [59] for both the top and anti-top quarks at 14 TeV. We quote the results for the case of the SM in table 3.

In figure 6 (upper panels), we plot the relative correction $\Delta P_i, i = x, y, z$ in the 2HDM type-I for the top quark in the $(m_{H^0},\, m_{A^0})$ plan. We see that ΔP_x reaches 2% as a maximum of enhancement. The suppression of P_x with respect to the SM value reaches -5%. Corrections to P_y are shown in the middle panel of figure 6, the corrections are rather smaller than those corresponding to P_x: $\max \Delta P_y \sim 0.5\%$ and the suppression is of

JHEP08(2016)082

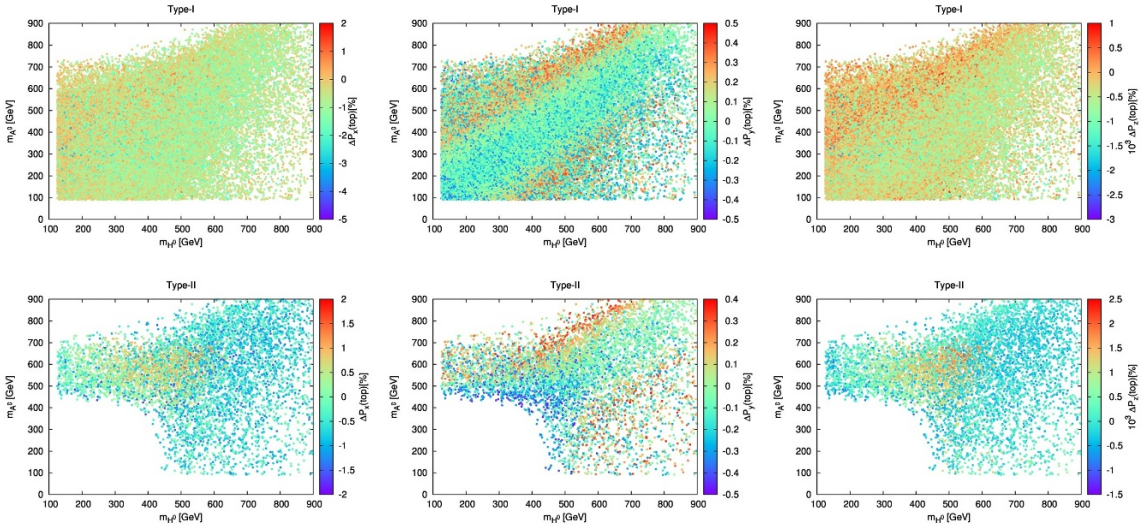

Figure 6. Scatter plots in (m_{H^0}, m_{A^0}) plan where the palette shows the values of ΔP_x (left panels), ΔP_y (middle panels) and ΔP_z (right panels) in the 2HDM type-I (upper panels) and 2HDM type-II (lower panels).

order of -0.5% which implies that non significant deviation from the SM is attained. We note also that the corrections to P_z (right panel of figure 6) are even more smaller (0.001% as a maximum).

In figure 6 (lower panels), we plot the relative corrections to the components of the polarization vector of the top in 2HDM type-II. We see that in this model, corrections are very small. $\max\{\Delta P_x, \Delta P_y, \Delta P_z\} = \{2\%, 0.4\%, 0.0025\%\}$ and $\min\{\Delta P_x, \Delta P_y, \Delta P_z\} = \{-2\%, -0.5\%, 0.0015\%\}$.

4.3 W helicity fractions

Anomalous tbW couplings could be probed by measuring the W boson helicity fractions in the top quark decay (unpolarized decay) [6, 7]. These polarization states are proven to be sensitive to new physics effects [8] where the W boson could be produced with positive (R), negative (L) or zero (0) helicity states, $\Gamma(t \to bW^+) = \Gamma_L + \Gamma_R + \Gamma_0$. Expressions of the polarized widths in terms of the anomalous couplings are taken from [40]. The polarization of the W boson could be measured by looking to the angular distributions of its decay products (especially into leptons). The differential decay rate of the unpolarized top quark is given by:

$$\frac{1}{\Gamma}\frac{d\Gamma}{d\cos\theta_l^*} = \frac{3}{8}(1+\cos\theta_l^*)^2 F_R + \frac{3}{8}(1-\cos\theta_l^*)^2 F_L + \frac{3}{4}\sin^2\theta_l^* F_0, \tag{4.3}$$

with $F_i = \Gamma_i/\Gamma$ are the helicity fractions and θ_l^* is the angle between the lepton three-momentum in the rest frame of the parent W boson and the W boson three momentum in the top quark rest frame. The SM predictions are known up to NNLO in QCD [57];

$$F_0 = 0.687 \pm 0.005, F_L = 0.311 \pm 0.005 \qquad \text{and} \qquad F_R = 0.0017 \pm 0.0001$$

JHEP08(2016)082

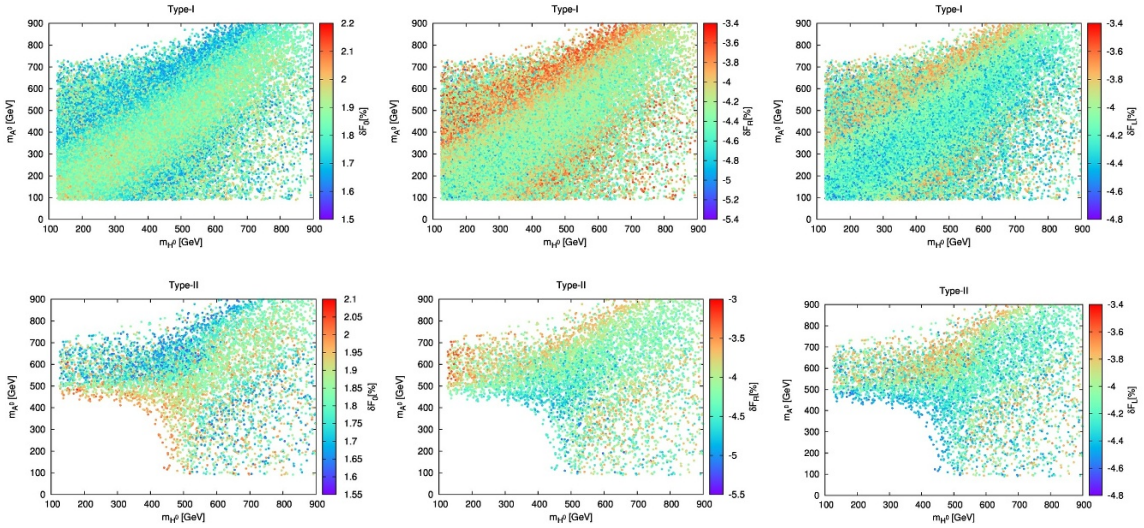

Figure 7. Scatter plot in the (m_{H^0}, m_{A^0}) plan where the palettes show the values of δF_0 (left panel), ΔF_R (middle panel) and ΔF_L (right panel) in the 2HDM type-I (top) and 2HDM type-II (bottom).

Calculations of the helicity fractions have been performed in the framework of the MSSM in [58].

For numerical analysis, we define the ratios δF_i by:

$$\delta F_i = \frac{F_i^{\rm 2HDM} - F_i^{\rm SM}}{F_i^{\rm SM}}, \tag{4.4}$$

where $F_i^{\rm SM}$ includes complete one-loop corrections (in α_s and α) while $F_i^{\rm 2HDM}$ contains additional the contribution from the extra particles of the 2HDM and its interference with the pure SM (EW and QCD) contribution.

In figure 7 (upper panels), we plot the contribution to the helicity fractions in 2HDM type-I. δF_0 is shown in the left-panel, where we observe that the corrections are quite small $\max \delta F_0 = 2.2\%$ and always enhancing F_0 with respect to its SM value while the minimum of the correction is 1.5%. Corrections to F_R is depicted in figure 7 (middle panel), we see that the corrections are always suppressing the SM value; $\max \delta F_R \sim -3.4\%$ and $\min \delta F_R \sim -5.4\%$. We notice that F_R is very small and vanishes in the limit $m_b \to 0$. We illustrate in the right panel of the same figure the correction to F_L. As it can be seen, there is always suppression of F_L with respect to its SM value $-4.8\% \leq \delta F_L \leq -3.4\%$.

In figure 7 (lower panels), corrections to F_i are shown in 2HDM type-II. In the left panel, we see that correction to F_0 is more or less of the same size as for the case of 2HDM type-I. The maximum of δF_0 is 2.1% reached where the masses are quite small $m_{H^0,A^0} \sim 300 - 400\,\text{GeV}$. In the middle panel of figure 7, we show the correction to F_R. We see that F_R is always suppressed with respect to its SM value. $-5.5\% \leq \delta F_R \leq -3\%$. Finally, the extra contribution to F_L is shown in the right panel of figure 7, one can see that the corrections are the same in 2HDM type-I and type-II, e.g $-4.8\% \leq \delta F_R \leq -3.4\%$ while the maximum of suppression is reached for the region of low scalar masses.

JHEP08(2016)082

5 Conclusion

We have computed the complete one loop contribution to the anomalous tbW couplings in the 2HDM. We give for the first time the analytical expressions of the anomalous couplings in terms of the Passarino Veltman functions. We have evaluated both the anomalous couplings g_L and g_R as well as left handed V_L and right handed V_R component of tbW. The computation is done by diagrammatic method in the Feynman gauge using dimensional regularization in the On-shell renormalization scheme.

We show sensitivity of the 2HDM parameters to the various anomalous tbW couplings taking into account recent LHC constraints. We also illustrate the overall sensitivity to the 2HDM parameters to some LHC observables such as: top polarization in single top production through t-channel as well as $W^{\pm}$ helicity fractions in top decay. We also project our numerical results on κ_D, which is the Yukawa coupling of the Higgs to down quarks and also on $\sin(\beta-\alpha)$ which leasure departure from decoupling limit of 2HDM.

The effect on most of the observales we consider are rather small. It will be rather a difficult task to disentangle the 2HDM from SM even with the High luminosity LHC option. However, with the projected Super B Factory experiments with high luminosity, from the precise measurement of $b \to s\gamma$ we would have a strong limit on V_R and g_L.

Acknowledgments

This work was supported by the Moroccan Ministry of Higher Education and Scientific Research MESRSFC and CNRST: "Projet dans les domaines prioritaires de la recherche scientifique et du développement technologique": PPR/2015/6. A.J would like to thank the STEP Programme (ICTP-Trieste) and GDRI P2IM Maroc-France (LAPTh, CNRS) for financial support during his stay where part of this work has been done. The authors would like to thank Fawzi Boudjema for careful reading of the manuscript.

A Anomalous tensor couplings in the SM

In this appendix, we give our numerical results for the anomalous tensor couplings in the SM and compare with results from [4] and [5].

In table 4 we show the values of g_L. In most of the cases, there is an agreement between our results and those presented by the authors of [4] except for diagrams with bW^+Z and bG^+Z exchange where our results are two times larger. On the other hand, in the diagrams with bW^+H and bG^+G^0 exchange, we have found that our imaginary part of g_L has a different sign to that found in [4].

In table 5, we show the values of coupling g_R for different diagrams and compares with the results of Vidal [4]. One can see that the same remarks apply here as for the case of tensor coupling g_L. In table 6, we show contribution to V_R for different diagrams in the SM and compare with the recent results of Vidal et al. reported in [5]. We have checked the correctness of our results, for certain diagrams where the results are not consistent with [4, 5], both by the Feynman parameterization and Passarino-Veltman reduction methods.

JHEP08(2016)082

Diagram	Contribution to g_L	Vidal et al. [4]
tZW^-	-0.0147	-0.0141
tG^0G^-	-0.00532	-0.0051
tG^-H	-0.010	-0.0088
tZG^-	-0.0016	-0.0012
$t\gamma W + t\gamma G^-$	-0.00925	-0.0094
bW^+Z	$-0.042 - 0.0457i$	$-0.0201 - 0.0214i$
bW^+H	$0.0089 + 0.0155i$	$0.0086 - 0.0120i$
bG^+G^0	$-0.0033 + 0.0172i$	$-0.0029 - 0.0167i$
bG^+H	$-0.000356 - 0.0138i$	$-0.0019 + 0.0111i$
bG^+Z	$-0.000765 - 0.000555i$	$-0.00039 - 0.00028i$
$bW^+\gamma + bG^+\gamma$	$-0.0262 + 0.0241i$	$-0.0270 + 0.0250i$
Ztb	-0.006846	-0.0067
γtb	0.011181	0.0115
G^0tb	-0.01134	-0.0109
Htb	-0.0162	-0.0153
$\Sigma(EW)$	$-0.128529 - 0.00330156i$	$-0.102 - 0.0014i$
gtb	-1.10326	-1.12

Table 4. A comparison between our results and those of [4] corresponding to $10^3 g_L$.

Diagram	Contribution to g_R	J. Vidal et al.
tZW^-	-1.211	-1.176
tHW^-	0.26147	0.220
tG^0G^-	-0.3644	-0.344
tG^-H	0.56	0.462
tZG^-	-0.02949	-0.050
$t\gamma W + t\gamma G^-$	0.5706	0.572
bW^+Z	$-1.33481 - 1.46899i$	$-0.623 - 0.664i$
bG^+G^0	$0.0001675 - 0.0011i$	$(1.5 + 11i) \times 10^{-4}$
bG^+H	$-0.000439 - 0.00117i$	$(-4.3 + 8.6i) \times 10^{-4}$
bG^+Z	$-0.1820 - 0.132i$	$-0.088 - 0.062i$
$bW^+\gamma + bG^+\gamma$	$0.118 - 0.503i$	$0.0114 - 0.509i$
Ztb	-0.4096	-0.397
γtb	0.0669	0.068
G^0tb	-0.00069	-6.8×10^{-4}
Htb	-0.00077	-6.2×10^{-4}
$\Sigma(EW)$	$-1.95628 - 2.10655i$	$-1.24 - 1.23i$
gtb	-6.60729	-6.61

Table 5. A comparison between our results and those of [4] correponding to $10^3 g_R$.

JHEP08(2016)082

Diagram	Contribution to V_R	Result of [5]
$tZW^{\pm}$	2.18162×10^{-5}	2.01×10^{-5}
$t\gamma W^{\pm}$	-1.22114×10^{-5}	-1.10×10^{-5}
$tHW^{\pm}$	0	0
$tG^{\pm}G^0 + tHG^{\pm}$	-1.67866×10^{-5}	-1.55×10^{-5}
$tZG^{\pm}$	0.117165×10^{-5}	0.1×10^{-5}
$t\gamma G^{\pm}$	0.76815×10^{-5}	0.69×10^{-5}
$bW^{\pm}Z$	$(1.19335 + 8.90489i) \times 10^{-4}$	$(1.12 + 8.24i) \times 10^{-5}$
$bW^{\pm}\gamma$	$(8.97983 - 4.71769i) \times 10^{-5}$	$(8.34 - 4.25i) \times 10^{-5}$
$bW^{\pm}H$	0	0
$bG^{\pm}G^0 + bG^{\pm}H$	$(1.05897 + 1.9014i) \times 10^{-5}$	$(1.01 - 0.35i) \times 10^{-5}$
$bG^{\pm}Z$	$(0.00109755 + 0.360717i) \times 10^{-5}$	$0.31i \times 10^{-5}$
$bG^{\pm}\gamma$	$(-4.82503 + 2.5363i) \times 10^{-5}$	$(-4.47 + 2.29i) \times 10^{-5}$
Ztb	-2.5271×10^{-5}	-2.30×10^{-5}
γtb	-2.98898×10^{-5}	-2.78×10^{-5}
$G^0tb + Htb$	-1.13206×10^{-5}	-1.03×10^{-5}
Σ(EW)	$(-0.0727959 + 8.98568i) \times 10^{-5}$	$(0.06 + 6.23i) \times 10^{-5}$
gtb	2.91224×10^{-3}	2.68×10^{-3}

Table 6. The right chiral coupling V_R in the SM at the one-loop order.

B Top quark anomalous couplings g_L, g_R and V_R in the Two-Higgs-Doublet-Model

In this appendix, we present for the first time the analytical expressions of the anomalous couplings for different diagrams in the 2HDM in terms of Passariono-Veltman functions. Here, κ_d^h, κ_d^H and κ_d^A are the Yukawa couplings defined in eq. (2.5) and in table 1. In the following, we mean by $C_{i,ij} = C_{i,ij}(m_b^2, m_t^2, M_W^2, m_A^2, m_B^2, m_C^2)$ the Passarino-Veltman functions, A, B and C are the particles running in the loops. $Q_b = 1/3, Q_t = 2/3$ and $C_F = 4/3$, $s_W = \sin\theta_W, c_W = \cos\theta_W, c_i = \cos i, s_i = \sin i$ and $t_i = \tan i$ where $i = \alpha, \beta$. Expressions in the case of the Standard Model are recovered by letting $s_{\beta-\alpha} \to 1, c_{\beta-\alpha} \to 0$ and $s_\beta = c_\alpha, s_\alpha = -c_\beta$ in the previous formulae.

B.1 Left tensorial coupling g_L

$$g_L^{bh^0t} = \frac{\alpha c_\alpha m_b m_t^2 \kappa_d^h}{16 M_W \pi s_\beta s_W^2}\{C_{12} - C_2\},$$
$$g_L^{bH^0t} = \frac{\alpha s_\alpha m_b m_t^2 \kappa_d^H}{16 M_W \pi s_\beta s_W^2}\{C_{12} - C_2\},$$
$$g_L^{A^0bt} = \frac{-\alpha m_b m_t^2 \kappa_d^A}{16 M_W \pi t_\beta s_W^2}\{C_{12} + C_{22}\},$$

$$g_L^{btG^0} = \frac{-\alpha m_b m_t^2}{16 M_W \pi s_W^2}\{C_1 + C_{12}\},$$

$$g_L^{bh^0H^\pm} = \frac{\alpha c_{\beta-\alpha} m_b \kappa_d^h}{16 M_W \pi s_W^2 t_\beta}\{m_b^2 t_\beta \kappa_d^A (C_0 - C_{11} - C_{12} + C_2) - m_t^2 (C_{12} + C_2 + C_{22})\},$$

$$g_L^{bH^0t} = \frac{\alpha s_\alpha m_b m_t^2 \kappa_d^H}{16 M_W \pi s_\beta s_W^2}\{C_{12} - C_2\},$$

$$g_L^{A^0bt} = \frac{-\alpha m_b m_t^2 \kappa_d^A}{16 M_W \pi t_\beta s_W^2}\{C_{12} + C_{22}\},$$

$$g_L^{btG^0} = \frac{-\alpha m_b m_t^2}{16 M_W \pi s_W^2}\{C_1 + C_{12}\},$$

$$g_L^{h^0H^\pm t} = \frac{\alpha c_\alpha c_{\beta-\alpha} m_b m_t^2}{16\pi M_W s_\beta t_\beta s_W^2}\{(-1 + t_\beta \kappa_d^A) C_{12} + t_\beta \kappa_d^A (2C_2 + C_{22})\},$$

$$g_L^{bh^0H^\pm} = \frac{\alpha c_{\beta-\alpha} m_b \kappa_d^h}{16 M_W \pi s_W^2 t_\beta}\{m_b^2 t_\beta \kappa_d^A (C_0 - C_{11} - C_{12} + C_2) - m_t^2 (C_{12} + C_2 + C_{22})\},$$

$$g_L^{H^\pm H^0 t} = \frac{-\alpha s_\alpha s_{\beta-\alpha} m_b m_t^2}{16\pi M_W s_\beta t_\beta s_W^2}\{(-1 + t_\beta \kappa_d^A) C_{12} + t_\beta \kappa_d^A (2C_2 + C_{22})\},$$

$$g_L^{bH^0H^\pm} = \frac{\alpha s_{\beta-\alpha} m_b \kappa_d^H}{16 M_W \pi s_W^2 t_\beta}\{m_b^2 t_\beta \kappa_d^A (-C_0 + C_{11} + C_{12} - C_2) + m_t^2 (C_{12} + C_2 + C_{22})\},$$

$$g_L^{A^0H^\pm t} = \frac{-\alpha m_b m_t^2}{16 M_W \pi s_W^2 t_\beta^2}\{(1 + t_\beta \kappa_d^A) C_{12} + t_\beta \kappa_d^A C_{22}\},$$

$$g_L^{A^0bH^\pm} = \frac{\alpha m_b \kappa_d^A}{16 M_W \pi s_W^2 t_\beta}\{m_b^2 t_\beta \kappa_d^A C_{11} + (m_t^2 + m_b^2 t_\beta \kappa_d^A) C_{12}\},$$

$$g_L^{h^0tG^\pm} = \frac{-\alpha c_\alpha m_b m_t^2 s_{\beta-\alpha}}{16 M_W \pi s_\beta s_W^2}\{2C_1 + C_{11} + 2C_{12}\},$$

$$g_L^{bh^0G^\pm} = \frac{-\alpha m_b s_{\beta-\alpha} \kappa_d^h}{16 M_W \pi s_W^2}\{m_b^2 (C_0 - C_{11} - C_{12} + C_2) + m_t^2 (C_{12} + C_2 + C_{22})\},$$

$$g_L^{H^0tG^\pm} = \frac{-\alpha s_\alpha m_b m_t^2 c_{\beta-\alpha}}{16 M_W \pi s_\beta s_W^2}(2C_1 + C_{11} + C_{12}),$$

$$g_L^{bH^0G^\pm} = \frac{-\alpha m_b c_{\beta-\alpha} \kappa_d^H}{16 M_W \pi s_W^2}\{m_b^2 (C_0 - C_{11} - C_{12} + C_2) + m_t^2 (C_{12} + C_2 + C_{22})\},$$

$$g_L^{tG^\pm G^0} = \frac{\alpha m_b m_t^2}{16 M_W \pi s_W^2}\{C_0 + C_{11} + C_{22} + 2(C_1 + C_{12} + C_2)\},$$

$$g_L^{bG^\pm G^0} = \frac{\alpha m_b}{16 M_W \pi s_W^2}\{m_b^2 (C_0 + C_1 + C_{12} + 2C_2 + C_{22}) + m_t^2 (C_1 + C_{11} + C_{12})\},$$

$$g_L^{\gamma bt} = \frac{Q_t Q_b \alpha m_b M_W}{2\pi}\{C_1 + C_{11} + C_{12}\},$$

$$g_L^{btZ} = \frac{\alpha m_b M_W (-3 + 4 s_W^2)}{72 c_W^2 \pi s_W^2}\{(-3 + 2 s_W^2)(C_{12} + C_{22}) + 2 s_W^2 C_2\},$$

$$g_L^{gbt} = \frac{-C_F \alpha_s m_b M_W}{2\pi}\{C_1 + C_{12} + C_{11}\},$$

JHEP08(2016)082

$$
\begin{aligned}
g_L^{\gamma bG^\pm} &= \frac{Q_b \alpha m_b M_W}{4\pi}\{C_0 + C_1 + C_2\},\\
g_L^{bG^\pm Z} &= \frac{-\alpha m_b M_W s_W^2}{12 c_W^2 \pi} C_2,\\
g_L^{h^0 tW} &= g_L^{H^0 tW} = 0,\\
g_L^{\gamma tG^\pm} &= \frac{-\alpha Q_t m_b M_W}{4\pi}\{C_0 + C_1 + C_2\},\\
g_L^{tG^\pm Z} &= \frac{\alpha m_b M_W(-3 + 4s_W^2)}{24 c_W^2 \pi} C_2,\\
g_L^{bh^0 W^\pm} &= \frac{\alpha m_b M_W s_{\beta-\alpha} \kappa_d^h}{8\pi s_W^2} C_2,\\
g_L^{bH^0 W^\pm} &= \frac{\alpha m_b M_W c_{\beta-\alpha} \kappa_d^H}{8\pi s_W^2} C_2,\\
g_L^{\gamma tW^\pm} &= \frac{Q_t \alpha m_b M_W}{4\pi}\{C_0 + C_1 - 2C_{12} - C_2\},\\
g_L^{\gamma bW^\pm} &= \frac{Q_b \alpha m_b M_W}{4\pi}\{-C_0 + C_1 + C_2 + 2(C_{11} + C_{12})\},\\
g_L^{tW^\pm Z} &= \frac{-\alpha m_b M_W(-3 + 4s_W^2)}{24\pi s_W^2}\{2C_{11} + 2C_{12} - C_2\},\\
g_L^{bZW^\pm} &= \frac{\alpha m_b M_W}{24\pi s_W^2}\{-(3 + 4s_W^2)C_1 + 2(3 - 2s_W^2)(C_{12} + C_{22}) - 6s_W^2 C_2\}
\end{aligned}
$$

B.2 Right tensorial coupling g_R

$$
\begin{aligned}
g_R^{bh^0 t} &= \frac{\alpha c_\alpha m_b^2 m_t \kappa_d^h}{16 M_W \pi s_\beta s_W^2}\{C_0 - C_{11} - C_{12} + C_2\},\\
g_R^{bH^0 t} &= \frac{\alpha s_\alpha m_b^2 m_t \kappa_d^H}{16 M_W \pi s_\beta s_W^2}\{C_0 - C_{11} - C_{12} + C_2\},\\
g_R^{A^0 bt} &= \frac{-\alpha m_b^2 m_t \kappa_d^A}{16 M_W \pi t_\beta s_W^2}\{C_{11} + C_{12}\},\\
g_R^{btG^0} &= \frac{\alpha m_b^2 m_t}{16 M_W \pi s_W^2}\{C_0 + C_1 + C_{12} + 2C_2 + C_{22}\},\\
g_R^{h^0 H^\pm t} &= \frac{\alpha c_\alpha c_{\beta-\alpha} m_t}{16\pi M_W s_\beta t_\beta s_W^2}\{(m_t^2 - m_b^2 t_\beta \kappa_d^A)C_{12} + m_t^2(2C_2 + C_{22})\},\\
g_R^{bh^0 H^\pm} &= \frac{-\alpha c_{\beta-\alpha} m_b \kappa_d^h}{16 M_W \pi s_W^2 t_\beta}\{-C_0 + C_{11} + C_{12} - C_2 + t_\beta \kappa_d^A(C_{12} + C_2 + C_{22})\},\\
g_R^{H^\pm H^0 t} &= \frac{-\alpha s_\alpha s_{\beta-\alpha} m_t}{16\pi M_W s_\beta t_\beta s_W^2}\{(m_t^2 - m_b^2 t_\beta \kappa_d^A)C_{12} + m_t^2(2C_2 + C_{22})\},\\
g_R^{bH^0 H^\pm} &= \frac{\alpha s_{\beta-\alpha} m_b^2 m_t \kappa_d^H}{16 M_W \pi s_W^2 t_\beta}\{-C_0 + C_{11} + C_{12} - C_2 + t_\beta \kappa_d^A(C_2 + C_{12} + C_{22})\},\\
g_R^{A^0 H^\pm t} &= \frac{\alpha m_t}{16 M_W \pi s_W^2 t_\beta^2}\{(m_t^2 + m_b^2 t_\beta \kappa_d^A)C_{12} + m_t^2 C_{22}\},
\end{aligned}
$$

JHEP08(2016)082

$$
\begin{aligned}
g_R^{A^0bH^\pm} &= \frac{-\alpha m_b^2 m_t \kappa_d^A}{16 M_W \pi s_W^2 t_\beta}\{C_{11} + (1 + t_\beta \kappa_d^A) C_{12}\},\\
g_R^{h^0tG^\pm} &= \frac{\alpha c_\alpha m_t s_{\beta-\alpha}}{16 M_W \pi s_\beta s_W^2}\{m_t^2(2C_1 + C_{11} + C_{12}) + m_b^2 C_{12}\},\\
g_R^{bh^0G^\pm} &= \frac{\alpha m_b^2 m_t s_{\beta-\alpha} \kappa_d^h}{16 M_W \pi s_W^2}\{C_0 - C_{11} + 2C_2 + C_{22}\},\\
g_R^{H^0tG^\pm} &= \frac{\alpha s_\alpha m_t c_{\beta-\alpha}}{16 M_W \pi s_\beta s_W^2}\{m_t^2(2C_1 + C_{11} + C_{12}) + m_b^2 C_{12}\},\\
g_R^{bH^0G^\pm} &= \frac{\alpha m_b^2 m_t c_{\beta-\alpha} \kappa_d^H}{16 M_W \pi s_W^2}\{C_0 - C_{11} + 2C_2 + C_{22}\},\\
g_R^{bG^\pm G^0} &= \frac{\alpha m_b^2 m_t}{16 M_W \pi s_W^2}\{C_0 + 2C_1 + C_{11} + 2C_{12} + 2C_2 + C_{22}\},\\
g_R^{\gamma bt} &= \frac{Q_t Q_b \alpha m_t M_W}{2\pi}\{C_2 + C_{22} + C_{12}\},\\
g_R^{btZ} &= \frac{-\alpha m_t M_W(-3 + 2s_W^2)}{72 c_W^2 \pi s_W^2}\{(-3 + 4s_W^2) C_{12} - 3C_2\},\\
g_R^{gbt} &= \frac{-C_F \alpha_s m_t M_W}{2\pi}\{C_2 + C_{12} + C_{22}\},\\
g_R^{\gamma bG^\pm} &= \frac{-Q_b \alpha m_t M_W}{4\pi}\{C_0 + C_1 + C_2\},\\
g_R^{bG^\pm Z} &= \frac{\alpha m_t M_W(-3 + 2s_W^2)}{24 c_W^2 \pi} C_2,\\
g_R^{h^0tW} &= \frac{\alpha c_\alpha m_t M_W s_{\beta-\alpha}}{8\pi s_\beta s_W^2} C_2,\\
g_R^{H^0tW} &= \frac{\alpha s_\alpha m_t M_W c_{\beta-\alpha}}{8\pi s_\beta s_W^2} C_2,\\
g_R^{\gamma tG^\pm} &= \frac{\alpha Q_t m_t M_W}{4\pi}\{C_0 + C_1 + C_2\},\\
g_R^{tG^\pm Z} &= \frac{-\alpha m_t M_W s_W^2}{6 c_W^2 \pi} C_2,\\
g_R^{bh^0W^\pm} &= g_R^{bH^0W^\pm} = 0,\\
g_R^{\gamma tW^\pm} &= \frac{Q_t \alpha m_t M_W}{4\pi}\{-C_0 + C_1 + C_2 + 2(C_{12} + C_{11})\},\\
g_R^{\gamma bW^\pm} &= \frac{Q_b \alpha m_t M_W}{4\pi}\{C_0 + C_1 - 2C_{12} - C_2\},\\
g_R^{tW^\pm Z} &= \frac{-\alpha m_t M_W}{24\pi s_W^2}\{(3 + 8s_W^2) C_1 - 2(3 - 4s_W^2)(C_{12} + C_{22}) + 12 s_W^2 C_2\},\\
g_R^{bZW^\pm} &= \frac{\alpha m_t M_W(-3 + 2s_W^2)}{24\pi s_W^2}\{-2(C_{11} + C_{12}) + C_2\}
\end{aligned}
$$

JHEP08(2016)082

B.3 Right chiral coupling V_R

$$
\begin{aligned}
V_R^{bh^0t} &= \frac{-\alpha c_\alpha m_b m_t \kappa_d^h}{16 M_W^2 \pi s_\beta s_W^2}\{-B_0(m_b^2, m_b^2, m_{h^0}^2)+2C_{00}+m_b^2(C_1+C_{11}+C_{12})+M_W^2(C_1+C_0+C_2)\\
&\quad +M_W^2(C_1+C_0+C_2)-m_t^2(C_1+C_0+C_{12})\},\\
V_R^{bH^0t} &= \frac{-\alpha s_\alpha m_b m_t \kappa_D^H}{16 M_W^2 \pi s_\beta s_W^2}\{-B_0(m_b^2, m_b^2, m_{h^0}^2)+2C_{00}+m_b^2(C_1+C_{11}+C_{12})+M_W^2(C_1+C_0+C_2)\\
&\quad -m_t^2(C_1+C_0+C_{12})\},\\
V_R^{A^0bt} &= \frac{-\alpha m_b m_t \kappa_d^A}{16 M_W^2 \pi s_W^2 t_\beta}\{-B_0(m_b^2, m_b^2, m_{A^0}^2)+2C_{00}-M_W^2 C_1+m_b^2(C_1-C_{11}-C_{12})\\
&\quad +m_t^2(C_1-C_{12}-2C_2-C_{22})\},\\
V_R^{btG^0} &= \frac{-\alpha m_b m_t}{16 M_W^2 \pi s_W^2}\{B_0(m_b^2, m_b^2, M_Z^2)-2C_{00}-m_b^2(C_{12}+C_2+C_{22})+m_t^2(C_0+C_{12}+C_2)\\
&\quad -M_W^2(C_0+C_1+C_2)\},\\
V_R^{h^0H^\pm t} &= \frac{\alpha c_\alpha c_{\beta-\alpha} m_b m_t}{16 M_W^2 \pi s_\beta s_W^2}\{t_\beta \kappa_d^A(2C_{00}+(m_t^2-m_b^2)C_{12})+m_t^2(1+\kappa_d^A t_\beta)(2C_2+C_{22})\},\\
V_R^{bh^0H^\pm} &= \frac{\alpha c_{\beta-\alpha} m_b m_t \kappa_d^h}{16 M_W^2 \pi t_\beta s_W^2}\{m_b^2((C_0-C_{11}-C_{12}-C_2)+t_\beta \kappa_d^A(C_0-C_{11}-2C_{12}-C_{22}))\\
&\quad -m_t^2(C_{12}+C_2+C_{22})\},\\
V_R^{H^\pm H^0 t} &= \frac{-\alpha s_{\beta-\alpha} s_\alpha m_b m_t}{16 M_W^2 \pi t_\beta s_\beta s_W^2}\{2t_\beta \kappa_d^A C_{00}+(m_t^2-m_b^2)t_\beta \kappa_d^A C_{12}+m_t^2(1+t_\beta \kappa_d^A)(2C_2+C_{22})\},\\
V_R^{A^0bH^\pm} &= \frac{\alpha m_b m_t \kappa_d^A}{16 M_W^2 \pi s_W^2 t_\beta}\{-2C_{00}+m_b^2(-1+\kappa_d^A t_\beta)C_{11}+(m_t^2-m_b^2)C_{12}\},\\
V_R^{h^0tG^\pm} &= \frac{\alpha c_\alpha m_b m_t s_{\beta-\alpha}}{16 M_W^2 \pi s_\beta s_W^2}\{-2C_{00}+(m_b^2-m_t^2)C_{12}\},\\
V_R^{bh^0G^\pm} &= \frac{\alpha s_{\beta-\alpha} m_b m_t \kappa_d^h}{16 M_W^2 \pi s_W^2}\{-2C_{00}+(m_b^2-m_t^2)(C_{12}+C_2+C_{22})\},\\
V_R^{H^0tG^\pm} &= \frac{\alpha c_{\beta-\alpha} m_b m_t s_\alpha}{16 M_W^2 \pi s_W^2 s_\beta}\{-2C_{00}+(m_b^2-m_t^2)C_{12}\},\\
V_R^{bH^0G^\pm} &= \frac{\alpha c_{\beta-\alpha} m_b m_t \kappa_d^H}{16 M_W^2 \pi s_W^2}\{-2C_{00}+(m_b^2-m_t^2)(C_{12}+C_2+C_{22})\},\\
V_R^{tG^\pm G^0} &= \frac{\alpha m_b m_t}{16 M_W^2 \pi s_W^2}\{2C_{00}+m_b^2(C_1+C_{11}+C_{12})+m_t^2(2C_0+3C_1+C_{11}+3C_{12}+4C_2+2C_{22})\},\\
V_R^{bG^0G^\pm} &= \frac{\alpha m_b m_t}{16 M_W^2 \pi s_W^2}\{2C_{00}+m_b^2(2C_0+3C_1+C_{11}+3C_{12}+4C_2+2C_{22})+m_t^2(C_1+C_{11}+C_{12})\},\\
V_R^{\gamma bt} &= \frac{Q_t Q_b \alpha m_b m_t}{2\pi}\{C_{11}+2C_{12}+C_{22}\},\\
V_R^{btZ} &= \frac{\alpha m_b m_t}{72\pi c_W^2 s_W^2}\{8s_W^4 C_0+2s_W^2(-9+8s_W^2)C_2+(9-18s_W^2+8s_W^4)C_{22}\},\\
V_R^{gbt} &= \frac{-C_F \alpha_s m_b m_t}{2\pi}\{C_{22}+2C_{12}+C_{11}\},\\
V_R^{bG^\pm\gamma} &= \frac{Q_b m_b m_t}{4\pi}C_1,\\
V_R^{bG^\pm Z} &= \frac{-\alpha m_b m_t s_W^2}{12 c_W^2 \pi}\{C_0+C_1+C_2\},\\
V_R^{th^0W^\pm} &= V_R^{tH^0W^\pm} = 0,
\end{aligned}
$$

JHEP08(2016)082

$$
\begin{aligned}
V_R^{\gamma t G^\pm} &= \frac{Q_t \alpha m_b m_t}{4\pi} C_1, \\
V_R^{t G^\pm Z} &= \frac{-\alpha m_b m_t s_W^2}{6 c_W^2 \pi} \{C_0 + C_1 + C_2\}, \\
V_R^{b h^0 W^\pm} &= V_R^{b H^0 W^\pm} = 0, \\
V_R^{\gamma t W^\pm} &= \frac{-Q_t \alpha m_b m_t}{4\pi} (C_1 - 2C_{11}), \\
V_R^{\gamma b W^\pm} &= \frac{-Q_b \alpha m_b m_t}{4\pi} \{C_1 - 2C_{11}\}, \\
V_R^{t W^\pm Z} &= \frac{\alpha m_b m_t}{12\pi s_W^2} \{-6 s_W^2 C_0 + (3 - 4 s_W^2)(C_{22} + C_{11} + 2C_{12}) + (3 - 10 s_W^2)(C_1 + C_2))\}, \\
V_R^{b W^\pm Z} &= \frac{\alpha m_b m_t}{12\pi s_W^2} \{-3 s_W^2 C_0 + (3 - 5 s_W^2)(C_1 + C_2) + (3 - 2 s_W^2)(C_{11} + 2C_{12} + C_{22})\}
\end{aligned}
$$

References

[1] D0 collaboration, S. Abachi et al., *Observation of the top quark*, *Phys. Rev. Lett.* **74** (1995) 2632 [hep-ex/9503003] [INSPIRE].

[2] CDF collaboration, F. Abe et al., *Observation of top quark production in $\bar{p}p$ collisions*, *Phys. Rev. Lett.* **74** (1995) 2626 [hep-ex/9503002] [INSPIRE].

[3] C.S. Li, R.J. Oakes and T.C. Yuan, *QCD corrections to $t \to W^+ b$*, *Phys. Rev.* **D 43** (1991) 3759 [INSPIRE].

[4] G.A. Gonzalez-Sprinberg, R. Martinez and J. Vidal, *Top quark tensor couplings*, *JHEP* **07** (2011) 094 [*Erratum ibid.* **1305** (2013) 117] [arXiv:1105.5601] [INSPIRE].

[5] G.A. González-Sprinberg and J. Vidal, *The top quark right coupling in the tbW-vertex*, *Eur. Phys. J.* **C 75** (2015) 615 [arXiv:1510.02153] [INSPIRE].

[6] CMS collaboration, *Measurement of the W-boson helicity in top-quark decays from $t\bar{t}$ production in lepton+jets events in pp collisions at $\sqrt{s} = 7$ TeV*, *JHEP* **10** (2013) 167 [arXiv:1308.3879] [INSPIRE].

[7] ATLAS collaboration, *Measurement of the W boson polarization in top quark decays with the ATLAS detector*, *JHEP* **06** (2012) 088 [arXiv:1205.2484] [INSPIRE].

[8] G.L. Kane, G.A. Ladinsky and C.P. Yuan, *Using the Top Quark for Testing Standard Model Polarization and CP Predictions*, *Phys. Rev.* **D 45** (1992) 124 [INSPIRE].

[9] W. Bernreuther, P. Gonzalez and M. Wiebusch, *The Top Quark Decay Vertex in Standard Model Extensions*, *Eur. Phys. J.* **C 60** (2009) 197 [arXiv:0812.1643] [INSPIRE].

[10] L. Duarte, G.A. González-Sprinberg and J. Vidal, *Top quark anomalous tensor couplings in the two-Higgs-doublet models*, *JHEP* **11** (2013) 114 [arXiv:1308.3652] [INSPIRE].

[11] B. Grzadkowski and M. Misiak, *Anomalous Wtb coupling effects in the weak radiative B-meson decay*, *Phys. Rev.* **D 78** (2008) 077501 [*Erratum ibid.* **D 84** (2011) 059903] [arXiv:0802.1413] [INSPIRE].

JHEP08(2016)082

[12] D0 collaboration, V.M. Abazov et al., *Combination of searches for anomalous top quark couplings with 5.4 fb^{-1} of $p\bar{p}$ collisions*, *Phys. Lett.* **B 713** (2012) 165 [arXiv:1204.2332] [INSPIRE].

[13] CMS collaboration, *W helicity in top pair events*, CMSPAS-TOP-11-020 (2012).

[14] J.A. Aguilar-Saavedra, J. Carvalho, N.F. Castro, A. Onofre and F. Veloso, *ATLAS sensitivity to Wtb anomalous couplings in top quark decays*, *Eur. Phys. J.* **C 53** (2008) 689 [arXiv:0705.3041] [INSPIRE].

[15] J.A. Aguilar-Saavedra, *Single top quark production at LHC with anomalous Wtb couplings*, *Nucl. Phys.* **B 804** (2008) 160 [arXiv:0803.3810] [INSPIRE].

[16] A. Prasath V, R.M. Godbole and S.D. Rindani, *Longitudinal top polarisation measurement and anomalous Wtb coupling*, *Eur. Phys. J.* **C 75** (2015) 402 [arXiv:1405.1264] [INSPIRE].

[17] A. Arhrib, F. Boudjema, R.M. Godbole and A. Jueid, *Probing anomalous Wtb couplings at the LHC*, to appear.

[18] S. Dutta, A. Goyal, M. Kumar and B. Mellado, *Measuring anomalous Wtb couplings at e^-p collider*, *Eur. Phys. J.* **C 75** (2015) 577 [arXiv:1307.1688] [INSPIRE].

[19] S.L. Glashow and S. Weinberg, *Natural Conservation Laws for Neutral Currents*, *Phys. Rev.* **D 15** (1977) 1958 [INSPIRE].

[20] M. Aoki, S. Kanemura, K. Tsumura and K. Yagyu, *Models of Yukawa interaction in the two Higgs doublet model and their collider phenomenology*, *Phys. Rev.* **D 80** (2009) 015017 [arXiv:0902.4665] [INSPIRE].

[21] G.C. Branco, P.M. Ferreira, L. Lavoura, M.N. Rebelo, M. Sher and J.P. Silva, *Theory and phenomenology of two-Higgs-doublet models*, *Phys. Rept.* **516** (2012) 1 [arXiv:1106.0034] [INSPIRE].

[22] N.G. Deshpande and E. Ma, *Pattern of Symmetry Breaking with Two Higgs Doublets*, *Phys. Rev.* **D 18** (1978) 2574 [INSPIRE].

[23] A.G. Akeroyd, A. Arhrib and E.-M. Naimi, *Note on tree level unitarity in the general two Higgs doublet model*, *Phys. Lett.* **B 490** (2000) 119 [hep-ph/0006035] [INSPIRE].

[24] S. Kanemura, T. Kubota and E. Takasugi, *Lee-Quigg-Thacker bounds for Higgs boson masses in a two doublet model*, *Phys. Lett.* **B 313** (1993) 155 [hep-ph/9303263] [INSPIRE].

[25] S. Kanemura and K. Yagyu, *Unitarity bound in the most general two Higgs doublet model*, *Phys. Lett.* **B 751** (2015) 289 [arXiv:1509.06060] [INSPIRE].

[26] Particle Data Group collaboration, K.A. Olive et al., *Review of Particle Physics*, *Chin. Phys.* **C 38** (2014) 090001 [INSPIRE].

[27] ATLAS collaboration, *Measurements of the Higgs boson production and decay rates and coupling strengths using pp collision data at $\sqrt{s} = 7$ and 8 TeV in the ATLAS experiment*, *Eur. Phys. J.* **C 76** (2016) 6 [arXiv:1507.04548] [INSPIRE].

[28] M. Baak et al., *Updated Status of the Global Electroweak Fit and Constraints on New Physics*, *Eur. Phys. J.* **C 72** (2012) 2003 [arXiv:1107.0975] [INSPIRE].

[29] T. Hermann, M. Misiak and M. Steinhauser, *$\bar{B} \to X_s\gamma$ in the Two Higgs Doublet Model up to Next-to-Next-to-Leading Order in QCD*, *JHEP* **11** (2012) 036 [arXiv:1208.2788] [INSPIRE].

[30] M. Misiak et al., *Estimate of $\mathcal{B}(\bar{B} \to X_s\gamma)$ at $O(\alpha_s^2)$*, *Phys. Rev. Lett.* **98** (2007) 022002 [hep-ph/0609232] [INSPIRE].

JHEP08(2016)082

[31] F. Mahmoudi and O. Stal, *Flavor constraints on the two-Higgs-doublet model with general Yukawa couplings*, *Phys. Rev.* **D 81** (2010) 035016 [arXiv:0907.1791] [INSPIRE].

[32] A. Freitas and Y.-C. Huang, *Electroweak two-loop corrections to $sin^2\theta^{b\bar{b}}_{eff}$ and R_b using numerical Mellin-Barnes integrals*, *JHEP* **08** (2012) 050 [*Erratum ibid.* **1305** (2013) 074] [arXiv:1205.0299] [INSPIRE].

[33] A. Denner, R.J. Guth, W. Hollik and J.H. Kuhn, *The Z width in the two Higgs doublet model*, *Z. Phys.* **C 51** (1991) 695 [INSPIRE].

[34] H.E. Haber and H.E. Logan, *Radiative corrections to the $Zb\bar{b}$ vertex and constraints on extended Higgs sectors*, *Phys. Rev.* **D 62** (2000) 015011 [hep-ph/9909335] [INSPIRE].

[35] M. Misiak et al., *Updated NNLO QCD predictions for the weak radiative B-meson decays*, *Phys. Rev. Lett.* **114** (2015) 221801 [arXiv:1503.01789] [INSPIRE].

[36] LEP, DELPHI, OPAL, ALEPH, L3 collaboration, G. Abbiendi et al., *Search for Charged Higgs bosons: Combined Results Using LEP Data*, *Eur. Phys. J.* **C 73** (2013) 2463 [arXiv:1301.6065] [INSPIRE].

[37] ATLAS collaboration, *Search for charged Higgs bosons in the τ+jets final state with pp collision data recorded at $\sqrt{s} = 8$ TeV with the ATLAS experiment*, ATLAS-CONF-2013-090 (2013).

[38] ATLAS collaboration, *Search for charged Higgs bosons decaying via $H^+ \to \tau\nu$ in top quark pair events using pp collision data at $\sqrt{s} = 7$ TeV with the ATLAS detector*, *JHEP* **06** (2012) 039 [arXiv:1204.2760] [INSPIRE].

[39] CMS collaboration, *Search for a light charged Higgs boson in top quark decays in pp collisions at $\sqrt{s} = 7$ TeV*, *JHEP* **07** (2012) 143 [arXiv:1205.5736] [INSPIRE].

[40] J.A. Aguilar-Saavedra, J. Carvalho, N.F. Castro, F. Veloso and A. Onofre, *Probing anomalous Wtb couplings in top pair decays*, *Eur. Phys. J.* **C 50** (2007) 519 [hep-ph/0605190] [INSPIRE].

[41] M. Fabbrichesi, M. Pinamonti and A. Tonero, *Limits on anomalous top quark gauge couplings from Tevatron and LHC data*, *Eur. Phys. J.* **C 74** (2014) 3193 [arXiv:1406.5393] [INSPIRE].

[42] Q.-H. Cao, B. Yan, J.-H. Yu and C. Zhang, *A General Analysis of Wtb anomalous Couplings*, arXiv:1504.03785 [INSPIRE].

[43] ATLAS collaboration, *Search for anomalous couplings in the Wtb vertex from the measurement of double differential angular decay rates of single top quarks produced in the t-channel with the ATLAS detector*, *JHEP* **04** (2016) 023 [arXiv:1510.03764] [INSPIRE].

[44] V. Cirigliano, W. Dekens, J. de Vries and E. Mereghetti, *Is there room for CP-violation in the top-Higgs sector?*, *Phys. Rev.* **D 94** (2016) 016002 [arXiv:1603.03049] [INSPIRE].

[45] V. Cirigliano, W. Dekens, J. de Vries and E. Mereghetti, *Constraining the top-Higgs sector of the Standard Model Effective Field Theory*, arXiv:1605.04311 [INSPIRE].

[46] J.L. Birman, F. Déliot, M.C.N. Fiolhais, A. Onofre and C.M. Pease, *New limits on anomalous contributions to the Wtb vertex*, *Phys. Rev.* **D 93** (2016) 113021 [arXiv:1605.02679] [INSPIRE].

[47] M. Böhm, H. Spiesberger and W. Hollik, *On the One Loop Renormalization of the Electroweak Standard Model and Its Application to Leptonic Processes*, *Fortsch. Phys.* **34** (1986) 687 [INSPIRE].

JHEP08(2016)082

[48] A. Denner, *Techniques for calculation of electroweak radiative corrections at the one loop level and results for W physics at LEP-200*, *Fortsch. Phys.* **41** (1993) 307 [arXiv:0709.1075] [INSPIRE].

[49] S. Dittmaier, *Separation of soft and collinear singularities from one loop N point integrals*, *Nucl. Phys.* **B 675** (2003) 447 [hep-ph/0308246] [INSPIRE].

[50] T. Hahn, *Generating Feynman diagrams and amplitudes with FeynArts 3*, *Comput. Phys. Commun.* **140** (2001) 418 [hep-ph/0012260] [INSPIRE].

[51] T. Hahn and C. Schappacher, *The Implementation of the minimal supersymmetric standard model in FeynArts and FormCalc*, *Comput. Phys. Commun.* **143** (2002) 54 [hep-ph/0105349] [INSPIRE].

[52] T. Hahn and M. Pérez-Victoria, *Automatized one loop calculations in four-dimensions and D-dimensions*, *Comput. Phys. Commun.* **118** (1999) 153 [hep-ph/9807565] [INSPIRE].

[53] J. Küblbeck, M. Böhm and A. Denner, *Feyn Arts: Computer Algebraic Generation of Feynman Graphs and Amplitudes*, *Comput. Phys. Commun.* **60** (1990) 165 [INSPIRE].

[54] G.J. van Oldenborgh, *FF: A Package to evaluate one loop Feynman diagrams*, *Comput. Phys. Commun.* **66** (1991) 1 [INSPIRE].

[55] T. Hahn, *Loop Calculations with FeynArts, FormCalc, and LoopTools*, *Acta Phys. Polon.* **B 30** (1999) 3469 [hep-ph/9910227].

[56] T. Hahn, *Feynman Diagram Calculations with FeynArts, FormCalc and LoopTools*, PoS(ACAT2010)078 [arXiv:1006.2231] [INSPIRE].

[57] A. Czarnecki, J.G. Korner and J.H. Piclum, *Helicity fractions of W bosons from top quark decays at NNLO in QCD*, *Phys. Rev.* **D 81** (2010) 111503 [arXiv:1005.2625] [INSPIRE].

[58] J.-j. Cao, R.J. Oakes, F. Wang and J.M. Yang, *Supersymmetric effects in top quark decay into polarized W boson*, *Phys. Rev.* **D 68** (2003) 054019 [hep-ph/0306278] [INSPIRE].

[59] J.A. Aguilar-Saavedra and S. Amor Dos Santos, *New directions for top quark polarization in the t-channel process*, *Phys. Rev.* **D 89** (2014) 114009 [arXiv:1404.1585] [INSPIRE].

JHEP08(2016)082